Long-Term Mechanical and Viscoelastic Behavior of Constitutive Polymeric Materials Used for Magnetic Tapes

BRIAN L. WEICK,[1] BHARAT BHUSHAN[2]

[1] School of Engineering, 3601 Pacific Avenue, University of the Pacific, Stockton, California 95211

[2] Computer Microtribology and Contamination Laboratory, Department of Mechanical Engineering, 206 W. 18th Avenue, The Ohio State University, Columbus, Ohio 43210

Received 14 August 2000; accepted 13 November 2000

ABSTRACT: Creep-compliance behavior of specially prepared magnetic tape materials was measured at elevated temperature levels to facilitate the use of a time–temperature superposition (TTS) process. This TTS process allowed for the construction of master curves at a reference temperature of 30°C, which were used to predict the long-term viscoelastic behavior of the magnetic particle (MP) and metal-evaporated (ME) tapes used in the study. The specially prepared samples allowed for the use of a rule of mixtures technique to determine the long-term creep compliance of the front coat and back coat used for the magnetic tapes. To test the validity of this procedure, the front coat, substrate, and back coat data determined through separate experiments were used to calculate creep compliances of simulated tapes. These calculated creep-compliance curves were then compared to measured data for the actual magnetic tapes. After determination and validation of the front coat, substrate, and back coat creep-compliance data sets, they were used to determine strain distributions when the tapes are stored in a reel. Strain distributions were calculated for two cases, which reflect how tapes are stored in different drives: (1) the front coat (magnetic + nonmagnetic layer) is oriented away from the hub, and (2) the front coat is oriented toward the hub. Results showed that strain in the critical front coat of a tape is lower if it is stored with the front coat oriented toward the hub. In addition, the use of the creep-compliance data showed that the MP tape front coat is more susceptible to creep than the ME tape front coat. The strain distributions in future magnetic tapes were also simulated by reducing the thickness and compliance of the layers. Results showed the importance of using lower compliance front coat, substrate, and back coat materials if thinner tapes are to be developed to increase the volume of information that can be stored in a magnetic tape reel. © 2001 John Wiley & Sons, Inc. J Appl Polym Sci 81: 1142–1160, 2001

Key words: viscoelasticity; compliance; creep; magnetic tapes; strain

INTRODUCTION

The information storage industry continues to develop and utilize advanced materials for magnetic tapes used in digital information systems, and flexible disks used in floppy and Zip® drives. In addition, the communication and recording industries rely on magnetic tapes to record and store audio and video information. To minimize deformation of polymeric materials used in the construction of flexible media for reliable performance of a product, properties and characteristics of the constitutive polymeric materials must be

Correspondence to: B. L. Weick.
Contract grant sponsor: CMCL (Ohio State University).

Journal of Applied Polymer Science, Vol. 81, 1142–1160 (2001)

measured and understood. Furthermore, predictive methods must be developed to assist designers with the development of future information storage products.

Magnetic tapes have properties and characteristics that must be understood in light of how they are used in a drive, and how they are stored in a reel. Thinner tape materials and higher areal densities (the product of linear and track densities) allow for an increase in the volume of information that can be stored using magnetic tapes. To make a magnetic tape with such high volumetric densities the substrate must be mechanically and environmentally stable with a high surface smoothness. For high track densities, lateral contraction of the constitutive tape materials from thermal, hygroscopic, viscoelastic, and/or shrinkage effects must be minimal. Lastly, various long-term reliability problems including uneven tape-stack profiles (or hardbands), mechanical print-through, instantaneous speed variations, and tape stagger problems can all be related to the viscoelastic characteristics of magnetic tape materials.[1]

Mechanical and viscoelastic characteristics of magnetic tapes and substrates have been determined by Bhushan[1] and Weick and Bhushan.[2–5] However, viscoelastic properties of the front coating and back coating alone are not as readily available. Such information is useful for designers wishing to develop future magnetic tapes that utilize thinner, lower compliance materials. Previous work by Weick and Bhushan[6] described a method for predicting the creep compliance of the constitutive layers of a magnetic tape. This work utilized creep data acquired at 50°C over a 50-h time period to predict the creep compliance of materials used for front and back coatings of magnetic tapes. Although this work was useful to predict short-term creep behavior of magnetic tapes exposed to an elevated design temperature of 50°C, it could not be used to predict long-term behavior of magnetic tapes at storage temperatures closer to ambient.

One of the objectives of the research presented herein is to develop and utilize methods for predicting the long-term behavior of front coats, substrates, and back coats used in typical magnetic tapes. Experimental creep data is presented for the (1) finished tape, (2) front coat + substrate with back coat removed, (3) substrate + back coat with front coat removed, and (4) substrate with front coat and back coat removed. Data sets obtained at 30, 50, and 70°C are presented. Time–temperature superposition is then used to predict the creep compliance of the materials tested at a reference temperature of 30°C. Master curves created at this reference temperature predict the long-term creep compliance of the tape, substrate, front coat + substrate, and substrate + back coat. A method known as the rule of mixtures is then used to predict the long-term creep compliance of the constitutive layers of a magnetic tape. Once the creep compliances for the front coat, substrate, and back coat are known, the properties and characteristics of future magnetic tapes are simulated using mathematical models written in the form of computer programs. The mathematical models are used to predict the long-term mechanical behavior of tapes based on the creep characteristics of each layer.

Due to the fact that magnetic tapes are stored in a reel, it is necessary to predict long-term behavior when the tapes are exposed to this combined state of stress. The tapes are subjected to applied tension, bending over a hub, and radial compression of the underlying layers. This leads to strain on the tape and associated lateral contraction. It is also important to show that the constitutive layers of the tape will be subjected to a different amount of strain depending on the compliance of each layer. This creep behavior is both temperature and time dependent, and when exposed to elevated temperatures over long periods of time, the constitutive layers of the magnetic tape will stretch and contract, leading to the long-term reliability problems discussed briefly herein, and discussed at length by Bhushan.[1]

Magnetic tapes are stored in a reel with either the front coat facing up or down. (In digital linear tape drives such as the TR5 the front coat is wrapped face up. The front coat is also wrapped face up in a Storage Technology 9840 drive; whereas in IBM 3490-type drives the front coat is wrapped face down.) The front coat consists of magnetic and nonmagnetic layers, and the deformation of these layers when stored in a reel can lead to problems reading information back from the tape. Strain distributions are therefore presented for both of these orientations. Furthermore, results are presented for both inner and outer wraps in the reel. These results show the increase in strain with time due to creep of the constitutive layers of the magnetic tape at a reference temperature of 30°C. Because the data sets are derived from time–temperature superposition experiments, creep compliances over a 1000 to 25,000-h time period could be predicted. In

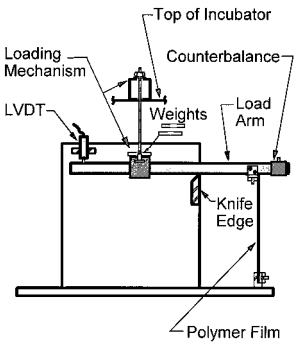

Figure 1 Schematic view of a creep tester for evaluating the creep behavior of magnetic tape materials.

addition, the strain distributions for future magnetic tapes with thinner, lower compliance layers are presented and discussed.

EXPERIMENTAL CREEP TESTING

Test Equipment

Creep-compliance measurements were made using the apparatus shown in Figure 1, which was developed by Bhushan[1] and Weick and Bhushan.[3] The magnetic tape specimens were tested simultaneously using this apparatus, which was placed in an incubator at the prescribed test temperature. The apparatus consisted of four balance beams (or load arms), and the test specimens were fixed at the end of each balance beam and aligned with a straight edge. A linear variable differential transformer (LVDT) was connected to the other end to measure deflection of the load arm due to creep of the test specimen, and the LVDT output was recorded on a PC. As shown in Figure 1, weights were placed on top of support pieces positioned around each load arm. Lowering or raising the support pieces was done remotely using a hand-driven lead screw mechanism after the incubator reached the preset test temperature.

Determination of Creep Compliance

During an experiment the LVDTs connected to each load arm measure the change in length of each magnetic tape test specimen. This change in length is in general a nonlinear function of time (and temperature) for polymers. The amount of strain the test specimen is subjected to can be calculated by normalizing the change in length of the specimen with respect to the original length. Creep compliance is then calculated by dividing the time-dependent strain by the constant applied stress:

$$\varepsilon(t) = \frac{\Delta l(t)}{l_o} \tag{1}$$

$$D(t) = \frac{\varepsilon(t)}{\sigma_o} = \frac{\Delta l(t)}{\sigma_o l_o} \tag{2}$$

where, $\Delta l(t)$ is the change in length of the test specimen as a function of time; l_o is the original length of the test specimen; $\varepsilon(t)$ is the amount of strain the film is subjected to; σ_o is the constant applied stress; and $D(t)$ is the tensile creep compliance of the test specimen as a function of time.

Creep-compliance data for the test specimens are modeled using a generalized Kelvin-Voigt model, which has the following mathematical form:

$$D(t) = D_o + \sum_{k=1}^{K} D_k[1 - \exp(-t/\tau_k)] \tag{3}$$

where D_o is the instantaneous compliance at time $t = 0$; D_k is the discrete compliance terms for each Kelvin-Voigt element; and τ_k is the discrete retardation times for each Kelvin-Voigt element.

Based on this model, for a constant stress of magnitude σ_o applied at $t = 0$, the instantaneous response of a viscoelastic solid will be a sudden strain of magnitude $\varepsilon_o = \sigma_o D_o$. This is followed by a delayed (or retarded) response, which can be attributed to the additional exponential terms in eq. (3). More specifically, each kth element of the model contributes a delayed compliance of magnitude D_k $[1 - \exp(-t/\tau_k)]$, and the amount of this delay is directly related to the magnitude of the retardation times τ_k.[7,8]

Equation (3) is typically represented as a series of parallel springs and dashpots connected to a single spring. This mechanical analog is shown in Figure 2, and is indicative of a viscoelastic poly-

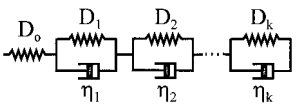

Figure 2 The Kelvin-Voigt model used to express the elastic and viscous characteristics of polymeric materials.

mer, which has an amorphous phase with mainly unoriented molecules, and a crystalline phase, which contains oriented molecules. Components of the polymeric structure, which respond instantly to an applied stress, are modeled as a single spring with an instantaneous compliance D_o. Components of the polymeric structure that do not respond instantly but are deformed in a time-dependent manner are modeled as multiple elements consisting of springs and dashpots acting in parallel. Each element contains a spring that has a compliance D_k, and a dashpot with a viscosity equal to η_k. The retardation time for each kth element is defined below:

$$\tau_k = \eta_k D_k \tag{4}$$

Note that the retardation time can also be interpreted as the length of time required to attain $(1 - 1/e)$ or 63.2% of the equilibrium strain for each element.[1,7–9]

Experimental data sets are fitted to eq. (3) using a nonlinear least-squares technique known as the Levenberg-Marquardt method.[10] This method is used to find the best-fit parameters τ_k and D_k for a Kelvin-Voigt model with multiple elements. Previous work by Weick and Bhushan[3] to determine the viscoelastic characteristics of alternative polymeric substrates used for magnetic tapes showed that two to three elements are typically required for a reasonable fit.

Experimental Procedure for Performing Creep Experiments

Prior to loading the samples, the incubator was turned on to stabilize the temperature in the chamber and allow the structure of the creep tester to undergo any dimensional changes. During this stabilization period of typically 3 h the signals from the LVDTs were monitored until they were steady. At this point the chamber was opened and the samples were fastened between the load arms and base of the creep tester. A preload of 0.5 MPa was applied to the specimens by adjusting the counterbalance weight on the load arm. The chamber was then closed and allowed to return to its preset temperature before beginning an experiment. After 3 h at 0.5 MPa, an additional 6.5 MPa stress was applied to the specimens using the external control mechanism for a total applied stress of 7.0 MPa. This relatively low stress has been shown to keep the creep experiments in the linear viscoelastic regime.[1,3] For the first hour, the sampling rate for the data acquisition system was set to 12.5 samples/second per load arm, and 25 data points acquired into memory were averaged for each data point written to the computer. After 1 h the sampling rate was slowed down to 0.25 samples/s with the same averaging scheme. Creep characteristics of the specimens were monitored for an additional 49 h. At the end of the 50-h experiment the sampling rate was once again increased to 12.5 samples/s per load arm, and the specimens were unloaded. Recovery characteristics were then monitored at the lower sampling rate for approximately 10 h or until the signals reached a steady level. Humidity was uncontrolled during the experiments, but was measured to be 25–30% during the 30°C experiments, less than 10% during the 50°C experiments, and 0% during the 70°C experiments.

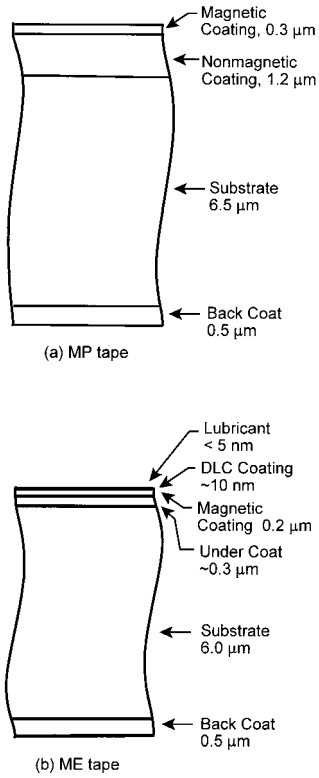

Figure 3 Schematic drawings of (a) Magnetic Particle (MP) tape (8.5 μm thick), and (b) Metal-Evaporated (ME) tape (7.0 μm thick). Both tapes are 6.35 mm wide. Tape thicknesses are drawn to scale.

Test Specimens

Magnetic tapes selected for this study are shown in Figure 3(a) and (b). These tapes are representative of the two basic types of magnetic tapes: (a)

particulate or MP tapes in which magnetic particles are dispersed in a polymeric binder, and (b) metal-evaporated or ME tapes in which continuous films of magnetic materials are deposited on to the substrate using vacuum techniques. Both tapes have ultrathin PET polyester substrates: 6.5 and 6.0 μm for the MP and ME tapes, respectively. The MP tape has an 0.3-μm magnetic layer with a 1.2-μm nonmagnetic layer, whereas the ME tape has a thinner 0.2-μm magnetic layer with an undercoat that is approximately 0.3 μm thick. Note that the ME tape also has a $<$5-nm thick lubricant and $\sim$ 10 nm diamond-like carbon (DLC) coating deposited on the magnetic layer. Both tapes have a 0.5-μm back coat. The total tape thickness for the MP tape is 8.5 μm, and the total tape thickness for the ME tape is 7.0 μm. Both tapes are 6.35 mm wide. The MP tape is used in Panasonic DVC Pro digital video cassettes, and is made by Fuji. The ME tape is used in Sony digital video cassettes.

Properties and characteristics of PET substrates have been well documented by Bhushan[1] and Weick and Bhushan.[2–5] PET used in the MP and ME tapes is tensilized for a high Young's modulus in the machine direction. The glass transition temperature of PET is typically 78°C. Information about the specific chemistry of the materials used in the front coats (magnetic plus nonmagnetic layers) and back coats is not available from the manufacturers. However, Weick and Bhushan[5] have discussed the types of materials typically used for MP and ME coatings. The MP coating for the Fuji tape consists of Fe metal alloy particles suspended in a polymeric binder consisting of vinylchloride copolymer, polyurethane, and polyisocyanate as a hardner. The MP coating is on top of a nonmagnetic layer. The continuous metal-evaporated coating for ME tapes is a dual layer of evaporated Co-O. Back coats for magnetic tapes are also comprised of organic polymers. The MP tape uses a nitrocellulose material for the back coat, but the material used for the ME tape is unknown.

Experiments Performed and Sample Preparation

All creep experiments discussed herein were performed at 30, 50, and 70°C for 50 h. These temperatures are below the glass transition temperature of PET ($\sim$ 78°C). To meet the objectives of this research, both MP and ME magnetic tape materials were used and the specific experiments performed are listed below: (1) magnetic tapes as-cut from the cassettes; (2) substrates + back coat (front coat removed); (3) substrates + front coat (back coat removed); and (4) substrates (front coat and back coat removed).

To obtain the substrate for the MP tape, methyl ethyl ketone (MEK) was used to remove the front coat and back coat. This involved placing the tape on a flat piece of glass and rubbing both sides of the tape longitudinally with a paper towel saturated with MEK until only the transparent PET substrate remained. The substrate for the ME tape was obtained in a similar manner. However, MEK could only be used to remove the back coat of the ME tape. A 2% hydrochloric acid solution was used to remove the front coat. This procedure involved dipping the ME tape in the solution until the metal-evaporated coating could be rubbed off.

Removing the back coat on the MP and ME tapes without removing the front coat involved spreading a thin bead of distilled water on a glass plate. The tape specimen was then placed front coat down in this bead of water. All excess water around the edges of the tape was soaked up with a paper towel. The back coat could then be carefully removed using MEK, and the thin film of polar water molecules between the glass plate and front coat of the tape helped prevent the nonpolar MEK molecules from dissolving the front coat. Removing the front coat on the MP and ME tapes without removing the back coat involved the same procedure.

DETERMINATION OF LONG-TERM CREEP-COMPLIANCE CHARACTERISTICS USING TIME–TEMPERATURE SUPERPOSITION

Methodology

An analytical technique known as time–temperature superposition (TTS) has been used to predict long-term creep behavior at ambient temperature.[8,11] For this analysis, creep measurements at elevated temperature levels are superimposed on one another to predict behavior at longer time periods. In the research presented herein, data sets acquired at 30, 50, and 70°C are superimposed at a reference temperature of 30°C to determine long-term creep behavior over an extended time period. The rationale behind this methodology stems from the observation that most polymers will behave in the same compliant manner at a particular high temperature as they

will when they are deformed at a particular slow rate at room temperature. In other words, there is a correspondence between time (or rate of deformation) and temperature.

Results and Discussion

Creep-Compliance Data at 30, 50, and 70°C

Data sets acquired for the MP and ME tape materials are shown in Figures 4 and 5. Results are presented for the 30, 50, and 70°C temperature levels for the following types of samples: (a) tape, (b) front coat + substrate material with back coat removed, (c) substrate + back coat with front coat removed, (d) substrate with front coat and back coat removed. The plots are shown on a log–log scale to accommodate the time–temperature superposition process used in the next step of the analytical process. Each experiment was performed for a duration of 50 h. For both the MP and ME tapes, an increase in temperature causes an increase in creep compliance. Furthermore, as indicated by the slopes of the creep-compliance curves, higher temperatures cause a higher rate of creep than lower temperatures. Note that the front coat + substrate and substrate + back coat data will be used in the TTS process and subsequently in the rule-of-mixtures process to determine the creep-compliance characteristics of the front and back coats alone. Therefore, these data sets will be discussed after completion of the data analysis.

It is useful to discuss and compare substrate and tape data for the MP and ME tapes. The overall creep compliance and rate of creep compliance for the substrates appear to be similar at

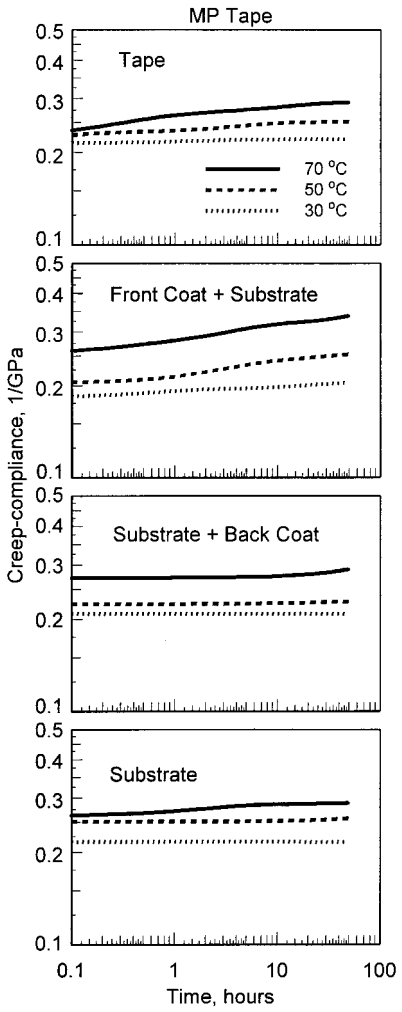

Figure 4 Creep-compliance data for MP tape materials at 30, 50, and 70°C.

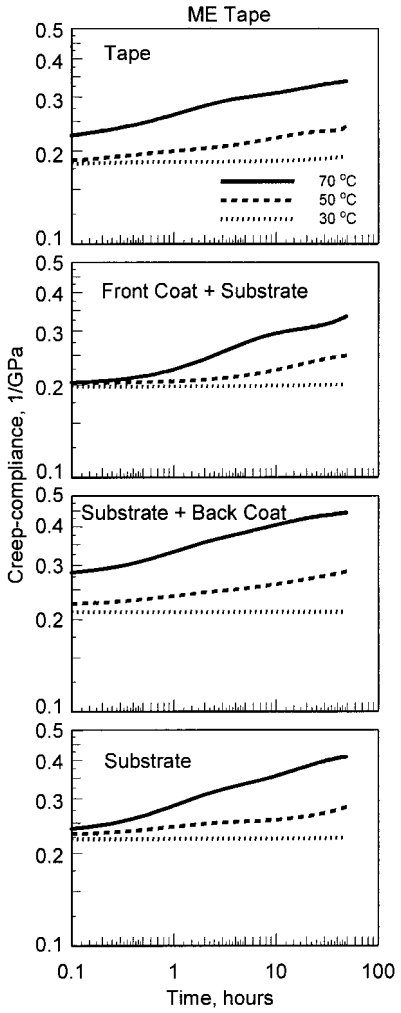

Figure 5 Creep-compliance data for ME tape materials at 30, 50, and 70°C.

30°C. This is not the case at higher temperatures. The substrate for the ME tape exhibits a higher overall creep rate than the substrate for the MP tape at 50 and 70°C. Therefore, even though both substrates are poly(ethylene terephthalate) or PET, there are differences between their creep-compliance behaviors. These differences could be attributed to manufacturing issues related to the orientation of the major optical axis and associated orientation of the macromolecules that comprise the polymer film.[1,3] Comparison of the tape data shows that the MP tape exhibits a slightly higher overall creep than the ME tape at 30°C. However, the slope of the curves at 50 and 70°C are higher for the ME tape. As stated previously, this trend is also observed in the other data sets for the ME tape, and could be attributed to the higher substrate-to-front coat thickness ratio of the ME tape when compared to the MP tape. Therefore, the creep-compliance behavior of the substrate could be dominating the creep-compliance behavior of the whole ME tape.

Creep-Compliance Master Curves at 30°C

The 30, 50, and 70°C data sets are superimposed on each other using the time–temperature superposition process to produce the master curves shown in Figures 6 and 7 for the MP and ME tapes, respectively. This superposition of the curves at a reference temperature of 30°C allows for the prediction of long-term creep-compliance behavior at this temperature over time periods as long as 10^6 h. Note that not all of the curves superimposed to the same extent. Therefore, some superimposed data sets can only be used to predict creep-compliance behavior out to between 10^4 and 10^5 h.

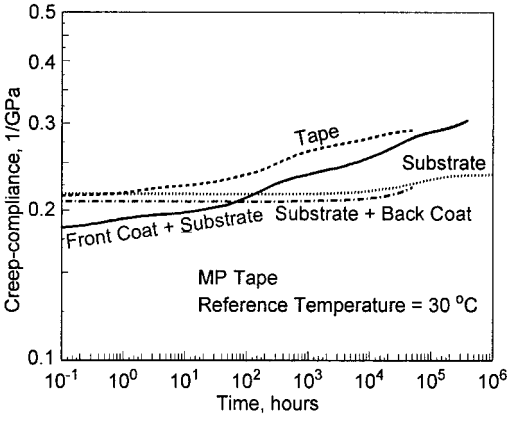

Figure 6 Creep-compliance master curves for MP tape materials at a reference temperature of 30°C.

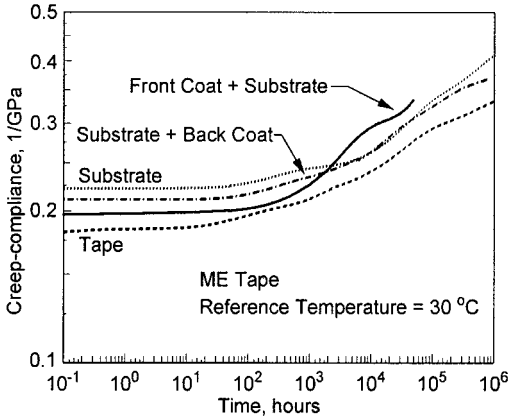

Figure 7 Creep-compliance master curves for ME tape materials at a reference temperature of 30°C.

Data sets for the substrate + back coat materials tested are similar to those determined for the substrates alone. This is due to the fact that the back coats are relatively thin, and play only a minor role in the creep behavior of the two layer substrate + back coat behavior. Note that the substrates exhibit a slightly higher creep compliance than the substrate + back coat materials. Therefore, the presence of the back coat, which is a nitrocellulose material for the MP tape, tends to lower the creep compliance of magnetic tapes.

The presence of front coats on a substrate tends to lower the creep compliance during the initial 100 to 200-h time period. This behavior is shown by both the MP and ME curves for the front coat + substrate materials. For the MP tape, the upward slope of the front coat + substrate line causes the creep compliance of this two-layer material to exceed that measured for the substrate after the 100-h time period. This upward trend continues, and could be attributed to presence of the binder used for the magnetic particle coating. For the ME tape, the initial lower creep compliance for the front coat + substrate material is expected due to the presence of the evaporated Co-O metal coating. However, this trend ends after about 200 h, and the creep compliance of the front coat + substrate increases for the ME tape. The cause of this increase is unknown, and will be addressed when the rule of mixtures is used to extract the front coat data.

The overall creep-compliance data of the MP tape is higher than the creep compliance of the ME tape at the 30°C reference temperature. Both

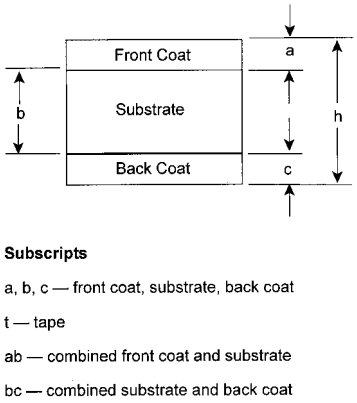

Figure 8 Nomenclature used for rule of mixtures equations.

tapes show an increasing trend to their creep compliance, and the ME tape appears to have a larger change in rate of creep as exhibited by the change in slope.

DETERMINATION OF CREEP-COMPLIANCE PROPERTIES OF CONSTITUTIVE LAYERS OF MAGNETIC TAPES

Methodology

Magnetic tapes are modeled as multiple layer polymer composite laminates consisting of a front coat, substrate and back coat. This model is depicted in Figure 8 along with pertinent nomenclature. Because magnetic tapes consist of a front coat (magnetic layer and nonmagnetic layer), substrate, and back coat, a rule of mixtures method is used to predict the creep compliance of a whole tape if the creep compliances of each layer are known. Jones[12] provides an excellent review of the rule of mixtures method, and Weick and Bhushan[6] demonstrated the applicability of this method for predicting the behavior of magnetic tapes at a temperature of 50°C over a relatively short 50-h time period. They also provide an extensive discussion of this methodology,[6] which will be summarized herein.

Equation (5) is used to determine the creep compliance of the front coat using data sets from creep-compliance experiments performed using a front coat + substrate material and a substrate material after the coatings have been removed (see Fig. 8 for nomenclature).

$$D_a(t) = \left[\left(\frac{a+b}{a} \right) \left(\frac{1}{D_{ab}(t)} \right) - \left(\frac{b}{a} \right) \left(\frac{1}{D_b(t)} \right) \right]^{-1} \quad (5)$$

Similarly, the creep compliance of the back coat is determined using data sets available from creep-compliance experiments performed using a substrate + back coat material and a substrate material.

$$D_c(t) = \left[\left(\frac{b+c}{c} \right) \left(\frac{1}{D_{bc}(t)} \right) - \left(\frac{b}{c} \right) \left(\frac{1}{D_b(t)} \right) \right]^{-1} \quad (6)$$

Once the creep compliances of the front coat and back coat are determined using eqs. (5) and (6), the creep compliance for a complete tape is predicted using eq. (7).

$$D_t(t) = \left[\frac{1}{h} \left(\frac{a}{D_a(t)} + \frac{b}{D_b(t)} + \frac{c}{D_c(t)} \right) \right]^{-1} \quad (7)$$

Data sets determined using eq. (7) for a complete tape utilize creep-compliance data for the front coat, substrate, and back coat from three separate experiments. To verify this technique, the data sets determined using eq. (7) are compared with actual measured data sets for a magnetic tape.

RESULTS AND DISCUSSION

Presentation of Results from Rule of Mixtures Calculations

Time–temperature superposition data for a reference temperature of 30°C are shown in Figures 9(a) and 10(a) for specimens prepared from the MP and ME tapes, respectively. These data sets are identical to those presented in Figures 6 and 7 for the front coat + substrate, substrate, and back coat + substrate. However, the range for the vertical axis has been extended to be consistent with other parts of Figures 9 and 10. Using the data sets shown in Figures 9(a) and 10(a), the rule of mixtures method summarized in eqs. (5) and (6) are used to predict the creep compliance of the front coat and back coat for each of the two tape materials. Figures 9(b) and 10(b) show the results when this method is applied. Front coat data were determined using eq. (5), back coat data were determined using eq. (6), and the substrate data sets from the actual experiments are plotted for reference. Finally, eq. (7) is used to determine the creep compliance of a simulated tape using the creep compliance determined for all three layers. These calculated data sets determined using the analytical model are compared to the measured

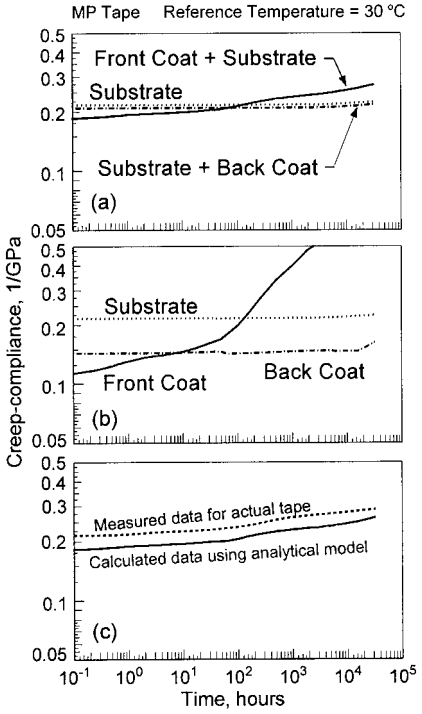

Figure 9 Creep compliances for an MP tape showing (a) experimental data, (b) front coat and back coat data determined using the rule of mixtures, and (c) comparison of calculated and measured creep compliances for the tape.

data for the actual tapes in Figures 9(c) and 10(c). These comparisons test the validity of the rule of mixtures method for extracting creep-compliance properties of the layers.

Discussion of Rule of Mixtures Results for Constitutive Layers of the MP Tape

Data sets presented in Figure 9(b) for the MP tape front coat and back coat show trends that are consistent with expectations. The back coat has a lower creep compliance than the substrate, and the front coat has a creep compliance that is initially lower than the creep compliance of the other layers. However, the rate of creep compliance of the front coat is comparatively large, and the creep compliance of this layer is higher than the other layers after the extended 10,000-h time period. As stated previously, the binder used for the magnetic layer is known to have elastomeric characteristics, and consists of polymers such as vinylchloride, urethane, and isocyanate polymers.[1] The detailed chemistry of this material is proprietary to the manufacturer, but the presence of the magnetic particles does not seem to keep the creep compliance at a low level at either the extended time periods, or the higher temperatures from which the extended time period data are derived. The properties of the binder appear to dominate the creep-compliance behavior of the front coat. Furthermore, the elastomeric characteristics of the front coat apparently causes that layer to be more susceptible to creep than the substrate. This is shown in Figure 9(b) by the large slope of the front coat line compared to the relatively low slope of the substrate line.

The back coat creep compliance is consistently lower than the substrate compliance. It is known that the manufacturer of the MP tape uses a nitrocellulose material for the back coat, which apparently has a lower creep-compliance behavior than the PET substrate. Creep of polymers is known to occur by secondary motions that involve the movement of main chain groups and/or side groups, and distortion through intermolecular distances.[3,9] Therefore, the type of chain groups, side groups, and strength of intermolecular bonding between polymer chains contributes to the creep process. Motions of side groups and intermolecular distortions contribute to the creep of

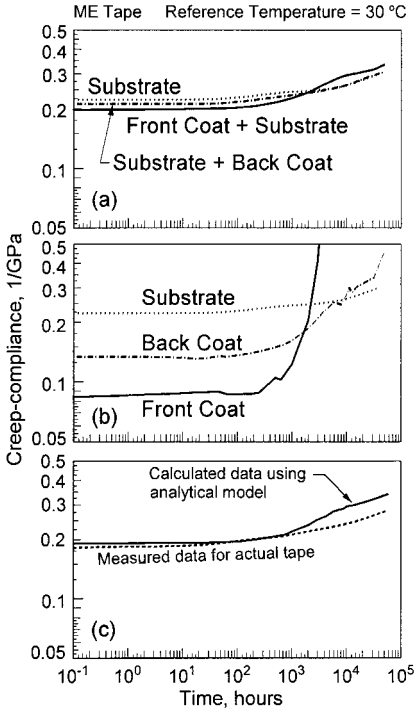

Figure 10 Creep compliances for an ME tape showing (a) experimental data, (b) front coat and back coat data determined using the rule of mixtures, and (c) comparison of calculated and measured creep compliances for the tape.

PET,[3] and these types of motions and distortions are apparently not as prevalent in the nitrocellulose material used for the back coat of the MP tape.

The validity of the MP tape front coat and back coat data is checked in Figure 9(c). Measured data for the actual tape are compared to analytical data calculated using eq. (7), and the front coat, substrate, and back coat data shown in Figure 9(b). Although there is a slight lower bias to the calculated data, the trend to the measured data and calculated data is similar.

Discussion of Rule of Mixtures Results for Constitutive Layers of the ME Tape

Front coat and back coat data determined using eqs. (5) and (6) are shown in Figure 10(b). For the initial 1000 h, the creep compliance of the front coat and back coat behave in a manner consistent with expectations. The front coat consists of a metal evaporated magnetic film deposited on a thin nonmagnetic layer. Due to the presence of this metallic layer, the creep compliance of the front coat is lower than the compliance of the substrate or back coat. The creep compliance of the back coat is also lower than the substrate for this initial time period. Although no information about the back coat is available from the manufacturer, it is likely to be a material similar to that used for the MP tape.

After about 1000 h, the creep compliance of the front coat increases significantly, and the compliance of the back coat also increases. It is unclear whether or not this sudden increase is realistic. When the calculated data are compared with the measured data in Figure 10(c), there is a close correspondence up to 1000 h. After that time period, the calculated data deviates from the measured data. Therefore, the behavior of the calculated front coat data after 1000 h is believed to be inconsistent with the actual creep behavior of this coating. Note that eq. (5) includes the thickness ratio term $(a + b)/(a)$, which is relatively large for ME tape due to the large thickness of the substrate compared to the front coat. Therefore, small changes in the creep compliance measured for the front coat + substrate can lead to large changes in the calculated creep compliance of the front coat. Referring back to Figures 7 and 10(a), the front coat + substrate data does increase after the 1000-h time period, and this measured data set is valid. However, the huge increase in the front coat creep compliance shown in Figure 9(b) is perhaps an overestimate of the actual behavior. For this reason, when strain distributions are calculated, data sets for the ME tape layers are used out to the 1000-h time period.

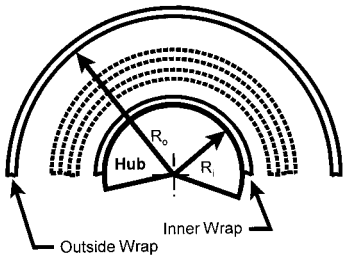

Figure 11 Schematic diagram showing tape segments wrapped around a hub.

DETERMINATION OF LONG-TERM STRAIN DISTRIBUTIONS IN THE CONSTITUTIVE LAYERS WHEN THE MAGNETIC TAPES ARE WOUND IN A REEL

Methodology

Due to the fact that magnetic tapes are wound in a reel for storage, they are subjected to stresses from applied tension, bending, and compression. A schematic diagram of a magnetic tape wound in a reel is shown in Figure 11. (Note that the term "wrap" will refer to the tapes located at the inner and outer parts of the tape stack as shown in Fig. 11. The term "layer" will continue to refer to the constitutive layers of the tape such as the front coat, substrate, and back coat as well as the magnetic and nonmagnetic layers which comprise the front coat.) Both inner and outside wraps are subjected to tensile stresses from applied tape tension. They are also subjected to bending stresses, and as shown in Figure 12 the inner wrap is subjected to a higher bending stress than the outside wrap due to a smaller radius of curvature. Furthermore, the inner wrap is subjected to radial compression from the rest of the tape stack. An equation for the total stress state follows:

$$\sigma(z) = \sigma_{\text{TENSION}} + \sigma_{\text{BENDING}} + \nu\sigma_{\text{RADIAL}} \qquad (8)$$

where, $\sigma(z)$ is the stress in the tape material in the x-direction as a function of distance from the hub (see Fig. 12); σ_{TENSION} is the stress in the tape due to applied tensile force; σ_{BENDING} is the stress in the tape due to bending over the hub;

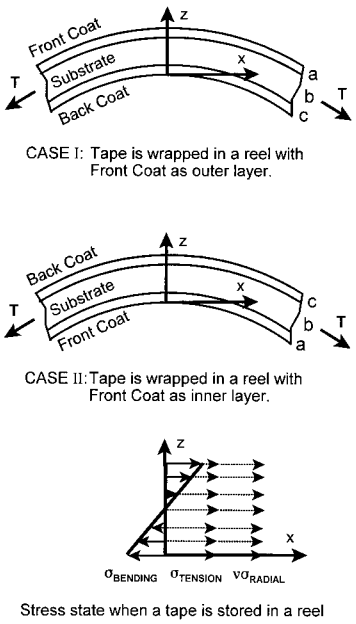

Figure 12 Stress distribution through a multiple layer magnetic tape when it is bent over a hub. Two different methods of wrapping the tape are shown: Case I—front coat up, and Case II—front coat down.

and $\nu\sigma_{\mathrm{RADIAL}}$ is the stress in the tape due to Poisson's component of the radial, compressive stress, where ν is the Poisson's ratio.

The tensile stress is assumed to be constant throughout the thickness of the tape, whereas the bending stress and Poisson's component of the radial stress are functions of z in eq. (8). Therefore, this equation is used to determine the combined stresses within each tape layer. Figure 12 provides a pictorial representation of this combined state of stress. This figure also depicts the two ways in which tapes are stored in a reel. Common double reel tape drives such as the TR5 store the tape with the front coat as the outer layer, which will be referred to as "front coat up." This is represented by Case I in Figure 12. In contrast, IBM 3490 drives store the tape with the front coat as the inner layer, which will be referred to as "front coat down." This is represented by Case II in Figure 12. Note that if the front coat faces up, it is subjected to the additive effects of tension, bending, and radial compression. If the front coat faces down, the bending stresses are in compression, and subtract from the total tensile stress state. A more detailed review of this stress model can be found in the previous work by Weick and Bhushan.[6]

Radius values of 10 and 30 mm are used to simulate the characteristics of an advanced Storage Technology 9840 tape drive, which has a hub radius of 11 mm, and an outer radius for the tape stack of 30 mm. Using this geometry, the total circumferential stress state for the MP and ME tapes is determined. The tensile stress in both tapes, $\sigma_{\mathrm{TENSION}}$, is held constant at 7.0 MPa. The component of the stress due to the Poisson's component of the radial stress, $\nu\sigma_{\mathrm{RADIAL}}$, is equal to 0.42 MPa at the inner wrap, and 0 at the outer wrap. The stresses due to bending, $\sigma_{\mathrm{BENDING}}$, range from 1.9 MPa at the inner wrap to 0.65 MPa at the outer wrap. Therefore, the tensile stress is predominant, and properties of the substrate remain important as new tapes with thinner front coats and substrates are developed.[6]

Once eq. (8) has been used to determine the stress distribution through a multiple layer magnetic tape, strain distributions are calculated using the compliance values determined for each layer. Referring to Figure 12, strain distributions for Case I (front coat up) are expressed as eqs. 9(a), (b), and (c), where h is the total thickness of the tape:

$$\varepsilon_a(z, t) = \sigma(z)D_a(t) \quad \text{circumferential strain in the front coat, } (b + c < z < h) \tag{9a}$$

$$\varepsilon_b(z, t) = \sigma(z)D_b(t) \quad \text{circumferential strain in the substrate, } (c < z < b + c) \tag{9b}$$

$$\varepsilon_c(z, t) = \sigma(z)D_c(t) \quad \text{circumferential strain in the back coat, } (z < c) \tag{9c}$$

For Case II (front coat down), the strain distributions are as follows:

$$\varepsilon_c(z, t) = \sigma(z)D_c(t) \quad \text{circumferential strain in the back coat, } (a + b < z < h) \tag{10a}$$

$$\varepsilon_b(z, t) = \sigma(z)D_b(t) \quad \text{circumferential strain in the substrate, } (a < z < a + b) \tag{10b}$$

$$\varepsilon_a(z, t) = \sigma(z)D_a(t) \quad \text{circumferential strain in the front coat, } (z < a) \tag{10c}$$

Equations (9) and (10) allow for the calculations of strain in each layer knowing the stresses and creep compliance for that layer. Note that the strain calculated is a function of z and time. The stress is assumed to be constant with time, which

is consistent with the definition of creep compliance in eq. (2).

The circumferential strain determined using eqs. (9) and (10) causes lateral strain on the tape. The ratio of lateral to circumferential strain is the Poisson's ratio, and a positive circumferential strain causes a negative lateral strain on the tape. Determination of lateral strain and associated lateral contraction is important for tape designers who have to consider track misregistration (TMR).[1–6] Weick and Bhushan[6] provide examples for tape designers who need to determine lateral strain and contraction for magnetic tapes.

Results and Discussion

Comparison of MP and ME Tape Strain Distributions

Case I: front coat up—strain distributions for the MP and ME tapes are shown in Figure 13 for Case I, which corresponds with the tape being wrapped with the front coat up as depicted in Figure 12. Note that strain distributions are shown for both the inner and outer wraps for each tape, and the inner wrap is assumed to be at a radius of 10 mm from the center of the hub with the outer wrap at a radius of 30 mm from the hub. The z axis is defined in Figure 12, and the 0-μm position is assumed to be at the bottom of each tape wrap. Because z is plotted as a function of strain in percent, the figures effectively show the cross-sectional strain distribution through the tape. Thicknesses are noted for each tape, and represent the thicknesses used to determine strain distributions for both the inner and outer wraps. Note that these plots do not account for the transitions between each layer. Equations (9) and (10) calculate the strain distributions for individual layers, but do not account for the interlayer strains. Therefore, discontinuities are present in the plots, which is consistent with the classical lamination technique from which this methodology is derived.[12]

Strain distributions determined using eq. (9) are shown in Figure 13 for a reference temperature of 30°C. For the MP tape, these strain distributions are shown at creep times of 1, 10, 100, 1000, and 25,000 h. For the ME tape, these strain distributions are shown at creep times of 1, 10, 100, and 1000 h.

Strain distributions for the MP tape show that the substrate and back coat are less susceptible to creep than the front coat. Furthermore, the strain in the back coat is typically less than the strain in

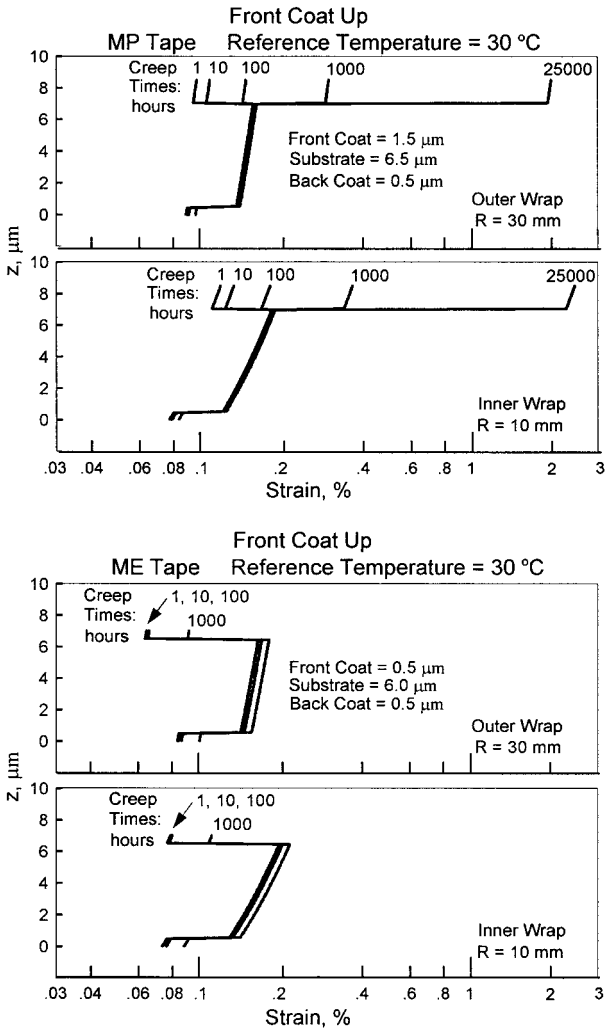

Figure 13 Strain distributions in MP and ME tapes when they are wound in a reel with the front coat up (Case I). Data sets are shown for both inner and outer wraps at a reference temperature of 30°C. The hub radius is assumed to be 10 mm, and the outer radius of the reel is assumed to be 30 mm.

the front coat and substrate at any given creep time. At the inner wrap, the strain in the substrate increases with distance from the hub, and this effect is less pronounced at the outer wrap. Front coat data show that at relatively short creep times of 1, 10, and 100 h, the strain on the front coat is lower than the strain on the substrate. However, as the creep time increases to 1000 and 25,000 h, the strain in the front coat increases substantially.

Results for the ME tape show that the strain distribution in the back coat and substrate is similar to what was observed for the MP tape, with a small increase in the effect of creep time on strain

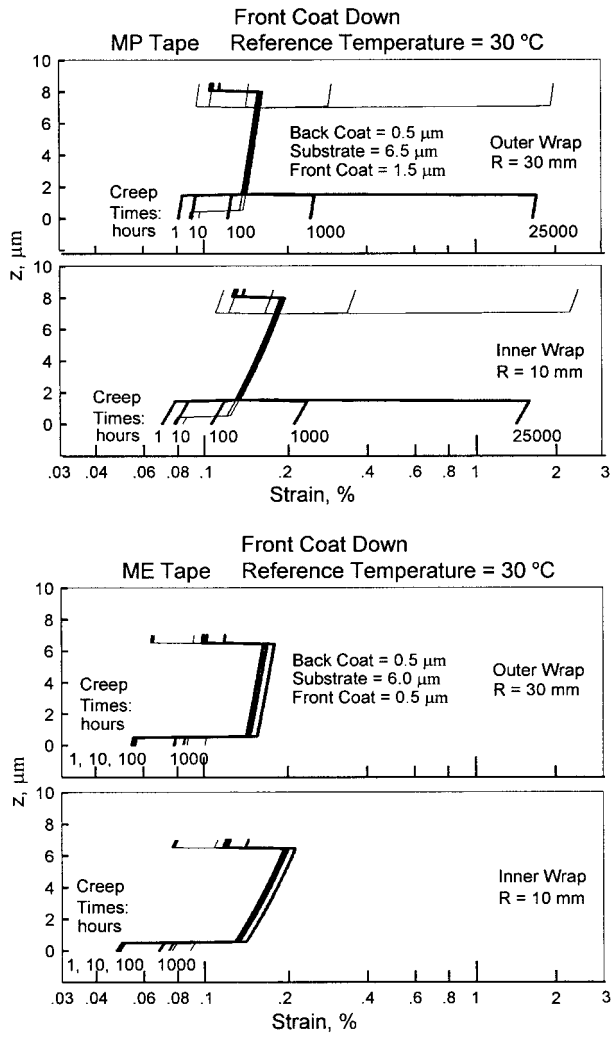

Figure 14 Strain distributions in MP and ME tapes when they are wound in a reel with the front coat down (Case II). Data sets are shown for both the inner and outer wraps at a reference temperature of 30°C. The hub radius is assumed to be 10 mm, and the outer radius of the reel is assumed to be 30 mm.

in these layers. However, the strain distributions in the front coat of the ME tape are less than what was observed for the MP tape. In addition, the strain in the front coat at the outer wrap is lower than the strain in the front coat at the inner wrap of the ME tape. At 1000 h, the strain in the front coat of the ME tape increases, but this increase is less than what was observed for the MP tape. The fact that the magnetic layer of the ME tape is a metal-evaporated film certainly plays a role in minimizing the strain in this layer.

Case II: front coat down—Figure 14 shows strain distributions generated for Case II in which the front coat is stored as the inner layer as shown in Figure 12. Recall that this situation is referred to as "front coat down." The strain distributions for Case II are shown as bold lines, and are superimposed on the strain distributions for Case I that were already presented separately in Figure 13. Consistent with how the underlying data sets were processed, the reference temperature is once again 30°C.

For both the inner and outer wraps of the MP and ME tapes, the strain in the front coat is reduced if it is stored down in the configuration prescribed by Case II. This is true at all creep times. Note that the strain in the back coat increases for the Case II configuration. The reduction in strain in the front coat and increase in strain in the back coat is a direct result of the presence of the bending stresses. Recall from Figure 12 that these bending stresses add to the tensile stresses at the outer layer of each wrap, but subtract from the tensile stresses at the inner layer of each wrap. Note that the strain distribution in the substrate is the same for Case I and II, which becomes obvious when one notes that eqs. 9(b) and 10(b) are identical. (However, the location of the substrate relative to the front coat and back coat is different in the two cases if the front coat is thicker than the back coat as is the case for the MP tape.)

Simulation of Strain Distributions in Thinner, Lower Compliance MP Tapes

Overview of simulations plotted for the MP tape: using the creep-compliance data sets determined for the front coat, substrate, and back coat, simulations can be performed to show the effects of reducing the thicknesses and compliances of the individual layers of a magnetic tape. Strain distributions are plotted as a function of tape thickness, and results for the MP tape are shown in Figure 15 for Case I in which the tape is wrapped with the front coat up. Results are shown in Figure 16 for Case II in which the tape is wrapped with the front coat down. In both Figures 15 and 16, graphs are shown for four different simulations: (1) substrate thickness reduced by $\frac{1}{3}$, (2) front coat and substrate thicknesses reduced by $\frac{1}{3}$, (3) compliance of front coat and substrate reduced by $\frac{1}{3}$, and (4) compliance and thickness of substrate and coatings reduced by $\frac{1}{3}$. Note that the bold-faced lines in the figures represent the simulations, and these simulations are superimposed on the actual strain distributions determined for the MP tape as shown in Figures 13 and 14 for Cases I and II, respectively.

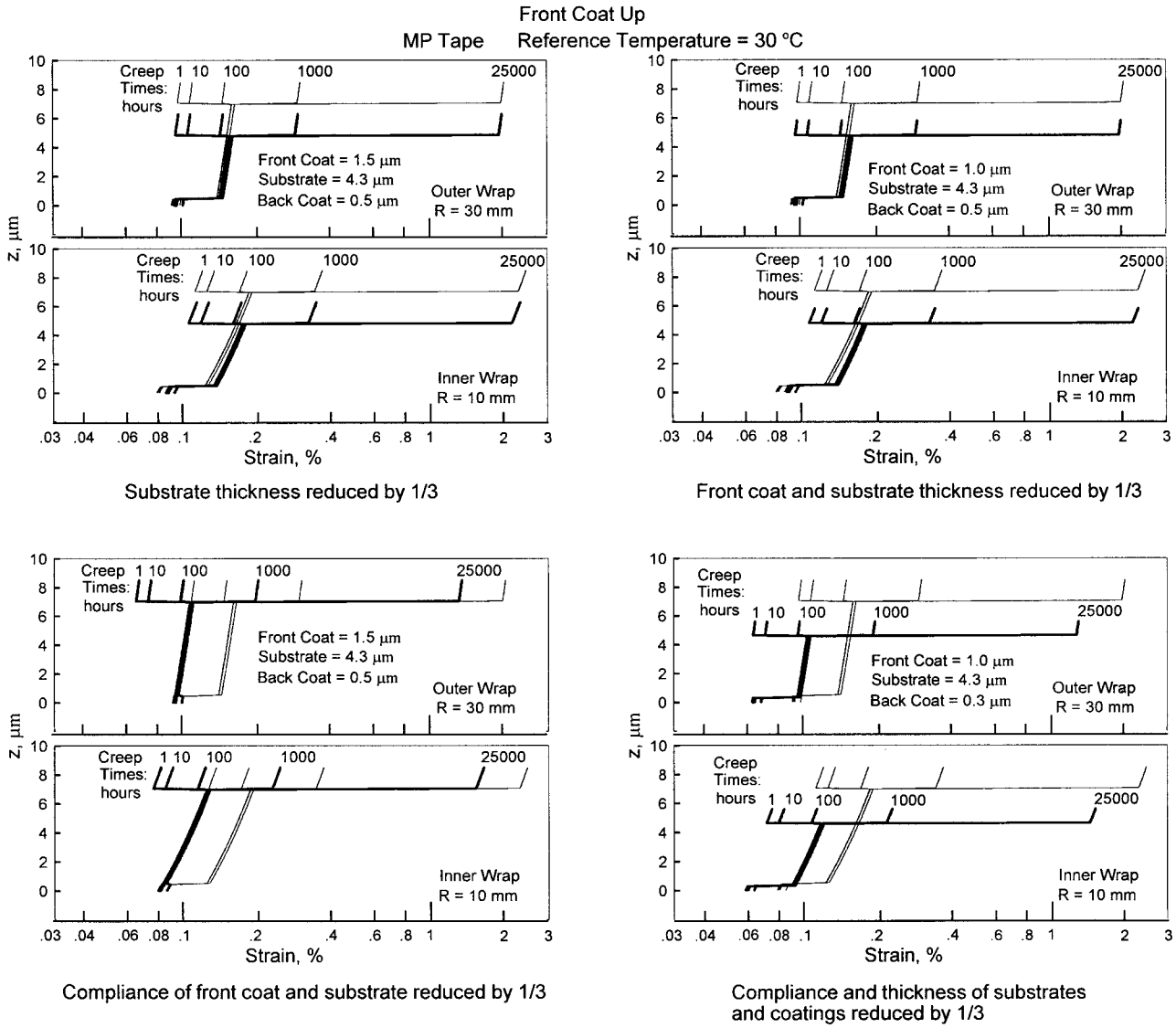

Figure 15 Strain distribution in an MP tape when it is wound in a reel with the front coat up (Case I). Data sets are shown for both the inner and outer wraps at a reference temperature of 30°C. The hub radius is assumed to be 10 mm, and the outer radius of the reel is assumed to be 30 mm.

Case I: front coat up: as shown in Figure 15, reducing the substrate and front coat thickness leads to a slight increase in strain on the substrate and back coat, with a slight decrease in strain on the front coat. Because the front coat of the MP tape is most susceptible to creep, it should be noted that the reduction in strain occurs at all creep times.

When the compliance of both the front coat and substrate is reduced by $\frac{1}{3}$, the strain in the front coat and substrate decreases more significantly. Note that strain in the front coat is reduced more significantly at the longer creep times of 1000 and 25,000 h than at the shorter creep times of 1, 10, or 100 h. At 25,000 h, the strain is reduced by approximately 0.7% if a lower compliance front coat and substrate are used; whereas at 1000, 100, 10, and 1 h, the reduction is approximately 0.1, 0.05, 0.038, and 0.034%, respectively. The strain in the substrate is reduced by approximately 0.05%.

When the compliance and thicknesses of both coatings and the substrate are reduced by $\frac{1}{3}$, an overall decrease in strain occurs. This decrease

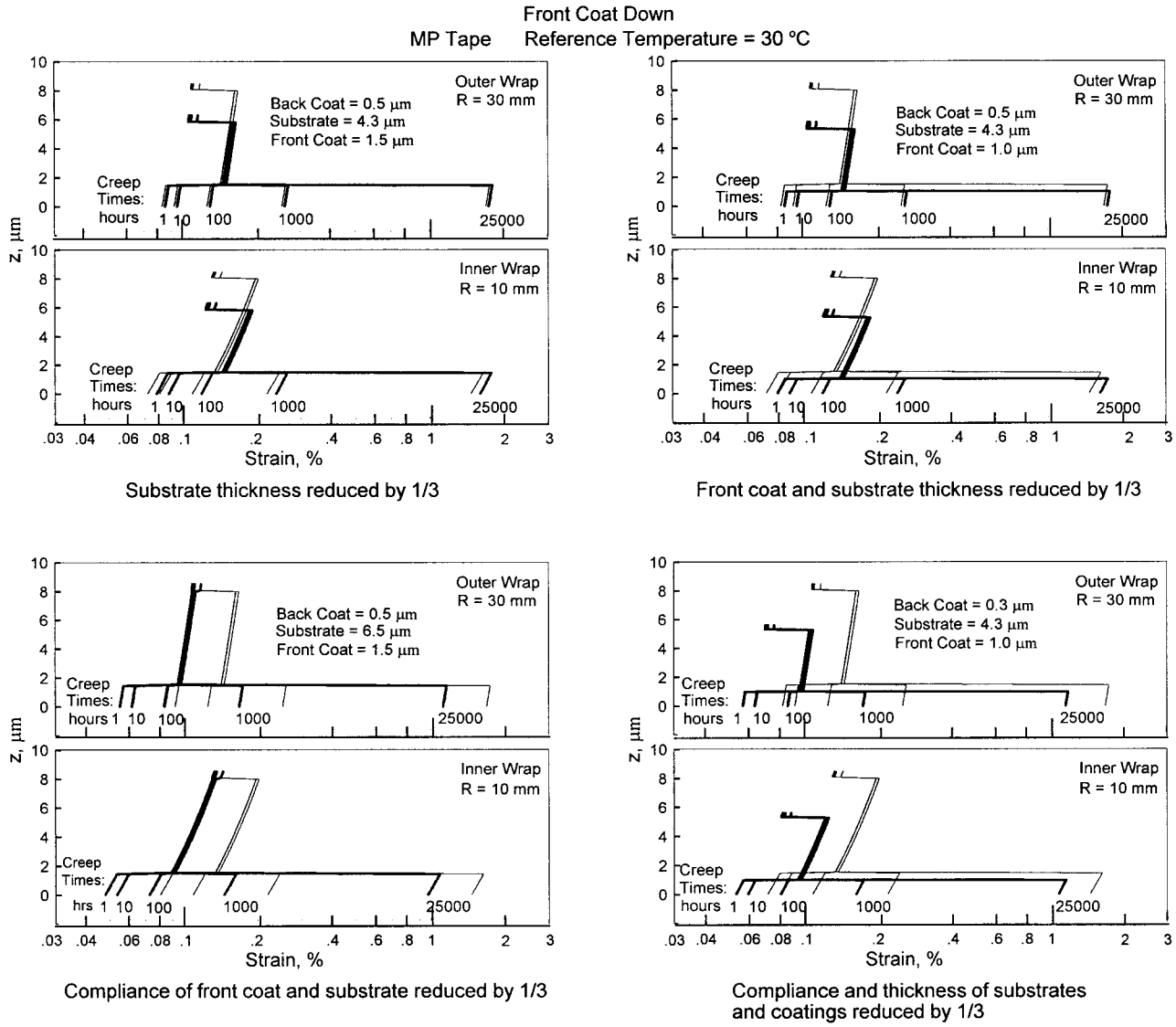

Figure 16 Strain distribution in an MP tape when it is wound in a reel with the front coat down (Case II). Data sets are shown for both the inner and outer wraps at a reference temperature of 30°C. The hub radius is assumed to be 10 mm, and the outer radius of the reel is assumed to be 30 mm.

appears to be approximately the same as when just the compliances are reduced. Therefore, it should be pointed out that reduction of creep compliance of the layers is necessary if future, thinner MP magnetic tapes are to be designed and manufactured for information storage applications.

Case II: front coat down: if the front coat is oriented down, there is a slight increase in strain on the front coat at all creep times if the thicknesses of the front coat and substrate are reduced. The upper two sets of graphs in Figure 16 show these results, and also show that the strain on the substrate will increase with a slight decrease in strain on the back coat.

Figure 16 also shows that reducing the creep compliance of the front coat and substrate by $\frac{1}{3}$ decreases the strain on the front coat and substrate. The extent of the decrease in strain is similar to what was observed in Figure 15 for Case I in which the front coat is oriented up. However, it should be pointed out that the overall strain level in the front coat is lower for Case II when compared to Case I. Figures 13 and 14

clearly presented this information because results for the two cases were superimposed on one another.

When the compliance and thickness of all the layers are reduced by $\frac{1}{3}$, the strain in the front coat, substrate, and back coat are all reduced. The extent of this reduction is slightly less than if the compliances are reduced without reducing the thicknesses. However, a reduction in compliance is necessary if thinner MP tape materials are to be used in advanced tapes. As shown in Figure 15, the same information was determined for Case I. Therefore, a reduction in compliance is needed if thinner MP tapes are to be manufactured regardless of whether or not they are stored with the front coat up or down.

Simulation of Strain Distributions in Thinner, Lower Compliance ME Tapes

Overview of simulations plotted for the ME tape: using the creep-compliance data sets determined for the front coat, substrate, and back coat, simulations can be performed to show the effects of reducing the thicknesses and compliances of the individual layers of a magnetic tape. Strain distributions are plotted as a function of tape thickness, and results for the ME tape are shown in Figure 17 for Case I in which the tape is wrapped with the front coat up. Results are shown in Figure 18 for Case II in which the tape is wrapped with the front coat down. In both Figures 17 and 18, graphs are shown for four different simulations: (1) substrate thickness reduced by $\frac{1}{3}$, (2) front coat and substrate thicknesses reduced by $\frac{1}{3}$, (3) compliance of front coat and substrate reduced by $\frac{1}{3}$, and (4) compliance and thickness of substrate and coatings reduced by $\frac{1}{3}$. Note that the bold-faced lines in the figures represent the simulations, and these simulations are superimposed on the actual strain distributions determined for the ME tape as shown in Figures 13 and 14 for Cases I and II, respectively. Lastly, the range for the strain axis used for the ME tape in Figures 17 and 18 is an order of magnitude less than the range used for the ME tapes in Figures 13 and 14. This was done to show the effects of thickness and compliance reduction more clearly.

Case I: front coat up: reducing the thickness of the substrate and front coat of the ME tape causes an increase in strain in the substrate and back coat with a slight decrease in strain in the front coat. These results are shown in Figure 17, and the effect of reducing the compliance of the front coat and substrate by $\frac{1}{3}$ is also shown in this figure. At the outer wrap, a reduction in compliance leads to an approximate 0.025% reduction in strain in the front coat at creep times of 1, 10, and 100 h. At a creep time of 1000 h, the reduction in strain is approximately 0.03% at the outer wrap. There appears to be a similar reduction in strain at the inner wrap when the compliance is reduced by $\frac{1}{3}$. When the thicknesses and creep compliances of all the layers are reduced, there is once again a reduction in strain in all layers of the tape. The same trend was observed for the MP tape, and leads to the same conclusion that a reduction in compliance must coincide with the reduction in thickness needed for future magnetic tapes.

Case II: front coat down: reduction of the thicknesses of the front coat and substrate leads to a slight increase in the strain in these layers if the front coat is oriented down. These data sets are shown in Figure 18. Note that the increase in strain is higher at the inner wrap than at the outer wrap. A reduction in compliance of the front coat and substrate leads to a decrease in strain in these layers, and a combined reduction in thickness and compliance is once again determined to be necessary if future ME tapes are to be manufactured.

SUMMARY AND CONCLUSIONS

Viscoelastic characteristics of representative magnetic tape materials have been evaluated using specially prepared samples. Creep-compliance properties were determined for the tapes, substrates, combined front coat + substrate and substrate + back coat materials. These properties were determined at elevated temperature levels, and time–temperature superposition (TTS) was used to construct master curves at a reference temperature of 30°C. These TTS curves show long-term viscoelastic behavior of the tape materials out to a time period of 10^6 h.

TTS data sets for the MP front coat + substrate samples evaluated in the study showed that the elastomeric binder used in the front coat of this tape is subjected to a higher rate of creep compliance than the other layers. Substrates for both the MP and ME materials showed creep behavior consistent with past work by the authors. Experiments involving the substrate + back coat showed creep behavior slightly lower than the substrate materials alone. Elevated temperature data sets and TTS results for the ME tape showed

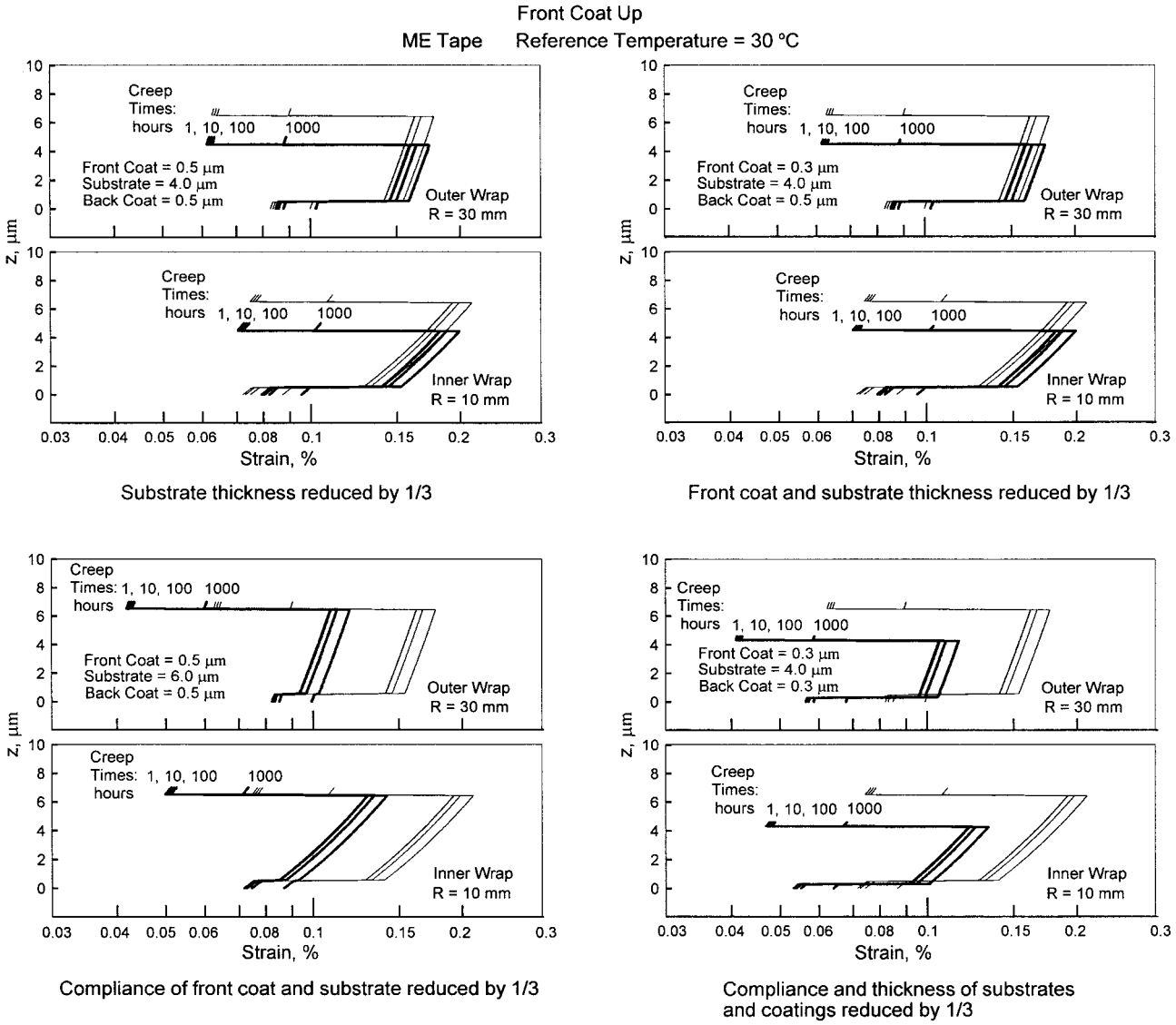

Figure 17 Strain distribution in an ME tape when it is wound in a reel with the front coat up (Case I). Data sets are shown for both the inner and outer wraps at a reference temperature of 30°C. The hub radius is assumed to be 10 mm, and the outer radius of the reel is assumed to be 30 mm.

that despite the presence of the metal-evaporated coating, the creep compliance of the ME tape appears to be dominated by the substrate. Although, at longer time periods the rate of creep compliance of the ME front coat + substrate apparently increases.

Using the TTS data sets, front coat + substrate and substrate + back coat data were used in the rule of mixtures methodology to determine long-term creep-compliance behavior of the front coat and back coat alone at a reference temperature of 30°C. The validity of the procedure was checked by using the rule of mixtures to determine calculated creep-compliance curves for the entire tape from the calculated front coat and back coat data. These calculated curves were compared with measured curves for the tapes themselves. The calculated MP tape curves proved to be consistent with the measured curves; whereas the ME calculated curves were only consistent with the measured curves out to a time period of 1000 h. After that time period, the calculated curve deviated significantly from the measured curves. Therefore, the ME front coat and back coat data were only used out to the 1000 h time period in determining strain distributions.

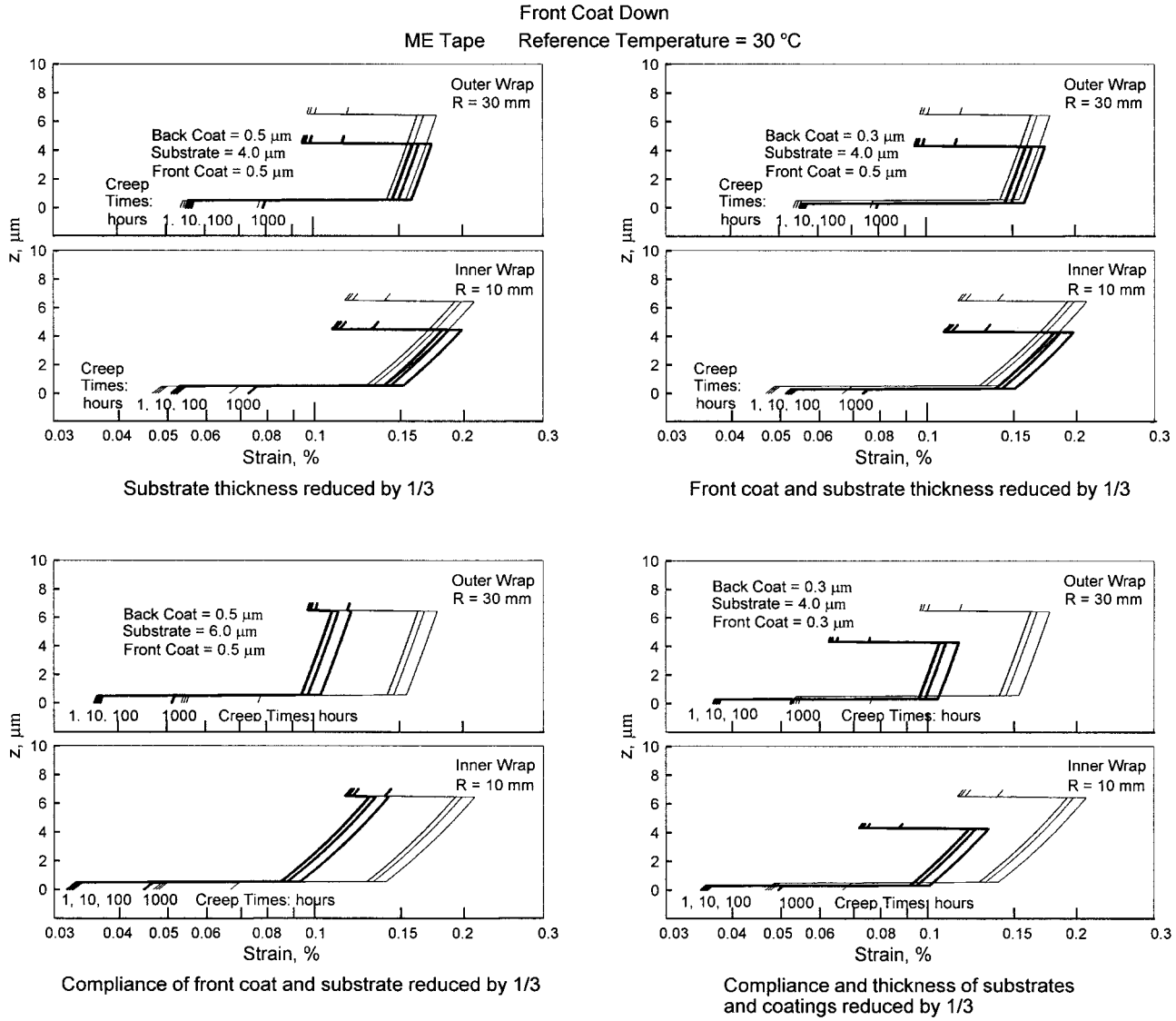

Figure 18 Strain distribution in an ME tape when it is wound in a reel with the front coat down (Case II). Data sets are shown for both the inner and outer wraps at a reference temperature of 30°C. The hub radius is assumed to be 10 mm, and the outer radius of the reel is assumed to be 30 mm.

Front coat data determined for the MP tape confirmed what was observed in the TTS plots of the front coat + substrate data. The creep compliance of the front coat shows an increasing trend throughout the long-term 10^4-h time period. This increasing trend could possibly be attributed to the binder materials such as vinyl chloride, urethane, isocyanate binder material used in the MP coating; however, detailed chemistry of this binder material is not available from the manufacturer. Back coat data determined for both the MP and ME tapes proved to be lower than the substrate creep compliance. Although the binder material is unknown for the ME tape, nitrocellulose is used for the MP tape back coat in this study. This nitrocellulose material apparently has fewer intermolecular distortions and side-chain movements, which are more prevalent in the PET substrate.

Strain distributions that occur when MP and ME tapes are wrapped in a reel were evaluated using the front coat and back coat data determined from the rule of mixtures and TTS methodologies. These distributions were determined through the thickness of the tape for two different cases. One case involved wrapping the tape with

the front coat oriented away from the hub (front coat up), and the other involved wrapping the tape with the front coat oriented toward the hub (front coat down). The front coat up orientation simulates how tapes are wrapped in double reel TR5 and Storage Technology 9840 drives; whereas the front coat down orientation simulates how tapes are wrapped in IBM 3490-type tape drives. Strain distributions were also simulated for future magnetic tapes, which will likely have thinner, lower compliance layers.

Wrapping the tapes with the front coat down proved to lower the overall the strain in the front coats of the tapes when compared to wrapping the tapes with the front coat up. Reducing the thickness of the constitutive layers of the tape proved to decrease the strain in the front coats slightly if the tapes are wrapped with the front coat up. For this same wrap method, decreasing the thickness actually caused an increase in strain in the substrate and back coat. If the tapes are wrapped with the front coat down, the strain in the front coat increases slightly, whereas the strain in the substrate and back coat decrease. Note that this behavior was observed for both the MP and ME tapes, but the front coat of the MP tape proved to be more susceptible to long-term strain than the front coat of the ME tape. However, data beyond the 1000-h time period could not be used for the ME tape.

Lower compliance materials for MP and ME tapes proved to be a necessity if future, thinner magnetic tapes are to be manufactured. Reducing the compliances of the layers caused a more significant decrease in strain than was observed when the thicknesses were reduced. Recall that in some cases, reducing the thickness without lowering the compliance actually caused an increase in strain in the layers of the tape. Also, tape designers often question whether or not to reduce the compliance of just the front coat or just the substrate. Based on results shown in Figures 15–18, it would appear that the compliances of both these layers need to be reduced. Furthermore, as demonstrated by reducing the thickness and compliances of all the layers, the reduction in compliance appears to be an important factor if strain and associated lateral contraction are to be minimized during long-term storage of magnetic tapes in a reel.

Support for this research was provided by the industrial membership of the Computer Microtribology and Contamination Laboratory (CMCL) at The Ohio State University. The creep apparatus at the University of the Pacific was developed and manufactured using funding from the UOP Faculty Research Committee. MP and ME tapes used in the study and useful information were generously supplied by Dr. K. Eljiri of Fuji (DVC PRO MP DP121) and by Dr. H. Osaki of Sony (Mini DV, DVM 60 Excellence), respectively.

REFERENCES

1. Bhushan, B. Mechanics and Reliability of Flexible Magnetic Media; Springer-Verlag: New York, 2000, 2nd ed.
2. Weick, B. L.; Bhushan, B. IEEE Trans Magn 1995, 31, 2937.
3. Weick, B. L.; Bhushan, B. J Appl Polym Sci 1995, 58, 2381.
4. Weick, B. L.; Bhushan, B. IEEE Trans Magn 1996, 32, 3319.
5. Weick, B. L.; Bhushan, B. In Encyclopedia of Electrical and Electronics Engineering; Webster, J. G., Ed.; Wiley: New York, 1999, p 226.
6. Weick, B. L.; Bhushan, B. J Info Storage Proc Syst 2000, 2.
7. Ferry, J. D. Viscoelastic Properties of Polymers; Wiley: New York, 1980, 3rd ed.
8. Tschoegl, N. W. The Phenomenological Theory of Linear Viscoelastic Behavior: An Introduction; Springer-Verlag: New York, 1989.
9. Aklonis, J. J.; MacKnight, W. J. Introduction to Polymer Viscoelasticity; Wiley: New York, 1983.
10. Press, W. H.; Flannery, B. P.; Teukolsky, S. A.; Vetterling, W. T. Numerical Recipes in C: The Art of Scientific Computing; Cambridge University Press: New York, 1988.
11. Williams, M. L.; Landel, R. F.; Ferry, J. D. J Am Chem Soc 1955, 77, 3701.
12. Jones, R. M. Mechanics of Composite Materials; Taylor & Francis: Philadelphia, 1999, 2nd ed.